Critical Properties for Carbon Dioxide + *n*-Alkane Mixtures Using a Variable-Volume View Cell

Eun-Joo Choi and Sang-Do Yeo*

Department of Chemical Engineering, Kyungpook National University, Taegu 702-701, Korea

Critical point data for carbon dioxide + hexane, + heptane, + octane, and + nonane were measured using a variable-volume view cell apparatus at mole fractions of carbon dioxide ranging from 0.974 to 0.834. Dew points and bubble points of the mixtures up to 395.7 K and 153.41 bar were measured by visual observation. The mixtures' critical points were determined by experimentally tracing the intersection point of the dew point and the bubble point loci on $P-T$ projections.

Introduction

High-pressure vapor−liquid equilibria of carbon dioxide + hydrocarbon systems have been widely investigated (Schneider, 1970). Phase behavior of carbon dioxide + *n*-alkane systems has been studied also at low temperatures (Im and Kurata, 1971). In this study, the critical points of carbon dioxide + hexane, + heptane, + octane, and + nonane binary mixtures were measured using a variable-volume view cell apparatus. The equipment allowed us to determine the critical points from both the dew point (DP) and bubble point (BP) lines by changing the pressure and temperature while maintaining a constant overall composition of the system. After the dew and bubble points of a constant-composition mixture were determined for a particular temperature, the measurement was repeated by narrowing the experimental condition toward the critical point region until the intersection point of the dew and bubble lines could be estimated. The critical point loci of binary mixtures containing low concentrations of *n*-alkanes were presented on $P-T$ projections.

Experimental Methods

Materials. Hexane, heptane, octane, and nonane with purities of 99.9% were purchased from Aldrich Chemical Co. and used without further purification. Carbon dioxide with a minimum purity of 99.9% was used in this study.

Apparatus and Procedure. The variable-volume view cell apparatus has been widely used to measure phase boundaries of high-pressure vapor−liquid equilibria. The equipment consisted of a view cell equipped with a window and a movable piston (stainless steel 316, 1.89 cm i.d., 6.35 cm o.d., 12.06 cm L), a pressure generator (HIP 81-5.75-10), a graduated volumetric flask (1500 cm^3), a borescope (Olympus F100-024-000-55), and a video monitor. The maximum volume of the cell used in this study was 26.71 cm^3. A detailed description of the apparatus can be found elsewhere (Chen and Radosz, 1992; Byun et al., 1996). The main feature of using the apparatus is that the phase transition pressure can be monitored at a constant composition and temperature. The pressure in the cell was measured using a pressure transducer (Cole Parmer E-68971-26) with an accuracy of ±0.6 bar, and the temperature was controlled within ±0.1 K.

A known mass of *n*-alkane was loaded into the cell. Carbon dioxide was charged to the cell, and the system was heated to the desired temperature. The system was pressurized by the movable piston, and the cell content was brought to one phase and left for 30 min with stirring used to obtain thermal equilibrium. The system pressure was decreased slowly using the pressure generator until a phase transition occurred. We observed the pressure at which the bright color through the window became cloudy, and this pressure was recorded as a phase transition point. Two different patterns of phase transition were observed: dew and bubble points. At dew point, we observed dew flowing down the window and a corresponding increase in the level of the lower phase. At bubble point, we observed bubbles ascending in the window and a corresponding decrease in the level of the lower phase.

The dew and bubble points were measured typically at every 5.0 K increase in the temperature range of 308.1−403.1 K, and the two adjacent dew and bubble points were located in a $P-T$ projection. Next, the temperature was changed in 0.2 K increments between the two adjacent points, and the phase transition patterns were again observed. This procedure was continued until we measured a dew point and a bubble point whose temperatures differed by less than the accuracy of this apparatus. Normally, the difference in temperatures and the corresponding phase transition pressures of each dew and bubble point pair were 0.2 K and 0.1 bar, respectively. Finally, the critical temperature and the critical pressure were determined by arithmetically averaging the two values of the dew and bubble points. After the measurement was completed, the cell content was vented through the graduated volumetric flask to determine the amount of carbon dioxide used. This enabled calculation of the mixture's composition within an accuracy of 1.5%.

Results

Figure 1 shows a typical $P-T$ diagram of a carbon dioxide + heptane binary mixture with a carbon dioxide mole fraction (x_A) of 0.904. The plot demonstrates the procedure for determining the critical point (CP) from the dew and bubble lines. The experimental methodology of this study was verified by measuring the critical point of the carbon dioxide/acrylic acid binary system that was previously conducted by Byun et al. (1996). Figure 2 shows the agreement between our result and the data in the

---

* To whom correspondence should be addressed. Email: syeo@bh.kyungpook.ac.kr.

S0021-9568(98)00029-6 CCC: $15.00

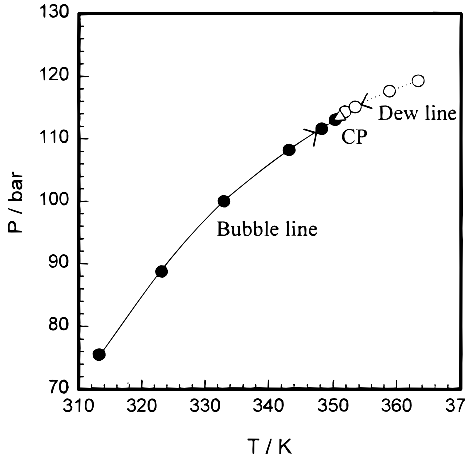

Figure 1. Phase transition boundary of a carbon dioxide + heptane mixture at carbon dioxide mole fraction of 0.904.

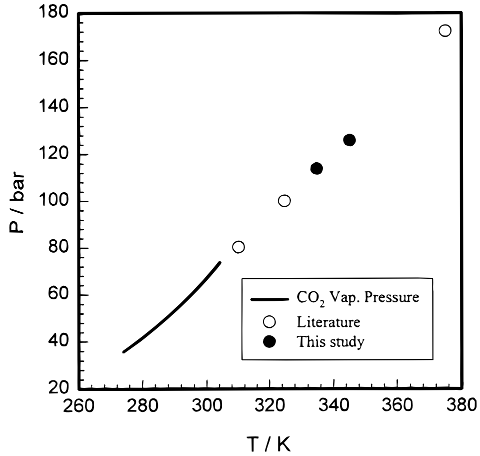

Figure 2. Critical point locus for carbon dioxide/acrylic acid binary mixtures. Literature data from Byun et al. (1996).

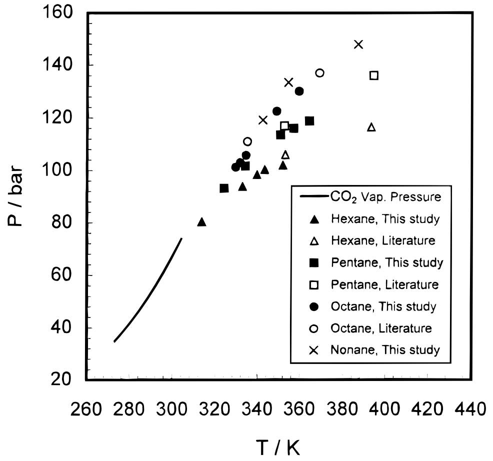

Figure 3. Critical point loci for carbon dioxide + hexane, + heptane, + octane, and + nonane binary mixtures. Literature data of hexane from Li et al. (1981), heptane from Kaira et al. (1978), and octane from Schneider (1970).

literature. The selected data of dew point, bubble point, and the evaluated critical point for the carbon dioxide + hexane, + heptane, + octane, and + nonane binary mixtures are listed in Table 1. Figure 3 shows the critical point loci of the carbon dioxide + *n*-alkane systems in a $P-T$ projection. The loci shifted to the left as the carbon number increased. The results agreed well with the data from the literature.

Table 1. Dew Point (DP), Bubble Point (BP), and Critical Point (CP) Data for Carbon Dioxide (A) + *n*-Alkane (B) Mixtures

x_A	T/K	P/bar	phase transition pattern	x_A	T/K	P/bar	phase transition pattern
			CO_2 (A) + Hexane (B)				
0.974	310.7	77.77	BP	0.880	358.2	106.73	DP
	312.9	79.84	BP	0.871	313.8	75.56	BP
	313.6	80.39	CP		328.1	89.73	BP
	314.4	80.94	DP		333.6	94.45	BP
0.922	313.1	77.49	BP		340.3	98.59	BP
	322.9	87.28	BP		343.0	99.97	BP
	328.3	91.32	BP		343.2	100.31	CP
	332.2	93.56	BP		343.4	100.66	DP
	332.6	93.87	CP		346.0	101.35	DP
	333.1	94.18	DP	0.834	313.7	75.29	BP
	343.5	97.69	DP		323.8	86.46	BP
0.880	314.3	71.84	BP		333.4	93.14	BP
	323.7	83.97	BP		343.4	98.87	BP
	333.7	94.04	BP		350.6	101.55	BP
	339.2	97.90	BP		351.8	101.97	CP
	339.5	98.38	CP		353.6	102.38	DP
	339.9	98.87	DP		355.1	103.00	DP
	347.7	102.04	DP		358.1	103.69	DP
			CO_2 (A) + Heptane (B)				
0.958	313.2	82.11	BP	0.904	351.7	114.03	DP
	317.9	86.80	BP		353.3	115.00	DP
	323.4	92.45	BP		363.3	119.14	DP
	324.0	93.04	CP	0.895	322.9	83.56	BP
	324.7	93.63	DP		342.9	105.14	BP
	327.9	95.97	DP		353.1	113.83	BP
0.925	328.7	95.97	BP		356.2	115.69	BP
	330.9	98.66	BP		357.0	115.97	CP
	332.3	100.18	BP		357.9	116.24	DP
	334.0	101.62	CP		363.1	119.55	DP
	335.7	103.07	DP		368.1	121.55	DP
	338.3	104.31	DP	0.885	323.6	85.49	BP
0.904	313.1	75.49	BP		343.1	107.69	BP
	323.1	88.73	BP		353.1	115.14	BP
	332.9	99.97	BP		363.3	118.57	BP
	343.1	108.17	BP		364.3	118.76	CP
	350.2	113.00	BP		365.3	118.93	DP
	350.7	113.52	CP		370.1	119.48	DP
			CO_2 (A) + Octane (B)				
0.958	313.1	81.90	BP	0.916	341.3	114.10	DP
	324.3	95.21	BP		348.1	119.07	DP
	328.8	100.52	BP	0.902	313.1	77.84	BP
	329.4	101.21	CP		323.3	93.21	BP
	330.1	101.90	DP		343.2	116.65	BP
	338.5	109.97	DP		348.1	122.10	BP
	342.9	112.93	DP		348.8	122.51	CP
0.939	313.1	76.87	BP		349.6	122.93	DP
	323.1	92.59	BP		358.1	129.96	DP
	329.3	100.31	BP		363.3	133.75	DP
	330.9	102.11	BP	0.878	313.1	76.53	BP
	331.6	102.93	CP		333.1	103.55	BP
	332.3	103.76	DP		343.1	113.90	BP
	338.4	106.79	DP		353.1	124.45	BP
0.916	313.1	76.87	BP		359.5	130.13	CP
	323.1	92.73	BP		360.3	130.93	DP
	333.1	104.45	BP		364.7	133.96	DP
	334.3	105.73	CP		368.1	135.55	DP
	335.5	107.00	DP				
			CO_2 (A) + Nonane (B)				
0.941	323.4	95.29	BP	0.925	355.3	134.31	DP
	333.1	108.18	BP		358.3	136.17	DP
	341.3	118.24	BP	0.878	322.7	91.42	BP
	342.3	119.18	CP		332.5	101.01	BP
	344.9	121.89	DP		353.5	121.00	BP
	347.8	124.86	DP		363.2	130.03	BP
	351.5	127.76	DP		382.5	144.44	BP
0.925	322.7	95.42	BP		386.8	147.96	CP
	333.1	108.73	BP		387.8	148.79	DP
	351.1	130.45	BP		392.8	151.89	DP
	353.5	132.72	BP		395.7	153.41	DP
	354.4	133.52	CP				

Literature Cited

Byun, H. S.; Hasch, B. M.; McHugh, M. A. Phase Behavior and Modeling of the Systems CO_2−Acetonitrile and CO_2−Acrylic Acid. *Fluid Phase Equilib.* **1996**, *115*, 179−192.

Chen, S. J.; Radosz, M. Density-Tuned Polyolefin Phase Equilibria. 1. Binary Solutions of Alternating Poly(ethylene−propylene) in Subcritical and Supercritical Propylene, 1-Butene, and 1-Hexene. Experiment and Flory-Patterson Model. *Macromolecules* **1992**, *25*, 3089−3096.

Im, U.K.; Kurata, F. Heterogeneous Phase Behavior of Carbon Dioxide in *n*-Hexane and *n*-Heptane at Low Temperatures. *J. Chem. Eng. Data* **1971**, *16*, 412−415.

Kaira, H.; Kubota, H.; Robinson, D. B.; Ng, H. Equilibrium Phase Properties of the Carbon Dioxide−*n*-Heptane System. *J. Chem. Eng. Data* **1978**, *23*, 317−321.

Li, Y. H.; Dillard, K. H.; Robinson, R. L. Vapor−Liquid Phase Equilibrium for Carbon Dioxide−*n*-Hexane at 40, 80, and 120 °C. *J. Chem. Eng. Data* **1981**, *26*, 53−55.

Schneider, G. M. Phase Equilibria in Fluid Mixtures at High Pressures. *Adv. Chem. Phys.* **1970**, XVII, 1−42.

Received for review January 23, 1998. Accepted May 15, 1998.

JE9800297